

1 **Simple and robust models of ecological abundance**

2

3 **John Alroy**

4

5 School of Natural Sciences, Macquarie University, NSW, Australia

6 Email: [john.alroy@mq.edu.au](mailto:john.alroy@mq.edu.au)

## 7 **Abstract**

- 8 1. Counts of species in ecological samples are of interest when they tell us about community  
9 assembly processes. Older process-based models of count distributions are either complex,  
10 widely rejected, or not able to predict high unevenness.
- 11 2. I leverage a general strategy for deriving simple one-parameter models. A distribution of  
12 abundances  $x$  on a continuous scale is predicted from a transform of a uniform distribution  $U$ ;  
13  $U$  is solved for to yield one minus a cumulative distribution function (CDF) for  $x$ ; and the  
14 result is differenced and rounded to down to yield a probability mass function. The same  
15 workflow has long been used to derive the geometric series from the exponential distribution.  
16 Three variants are proposed, respectively based on the transforms  $\mu/U - \mu = (\mu - U)/U$  where  
17  $\mu$  is a fitted constant (a scaled odds);  $[-\ln(U)/\lambda]^2$  where  $-\ln U$  is just an exponential random  
18 variate and  $\lambda$  is the constant; and  $[-\ln(2/U - 1)/\gamma]^4$  where  $\gamma$  is the constant. They collectively  
19 cover the range of functions that lead from some  $U$  to a non-negative real number.
- 20 3. The distributions are all consistent with simple population dynamical models in which  
21 recruitment rates, and sometimes death rates, vary randomly amongst species and are fixed  
22 for each species. The number of recruited offspring produced during each interval by each  
23 species is Poisson-distributed, and death rates are per-capita. Population counts are  
24 equilibrial, allowing co-existence in the absence of competition.
- 25 4. Large-scale surveys of corals, fishes, butterflies, and trees are consistent with the  
26 distributions, as are local-scale inventories of trees and assorted vertebrate and insect groups.  
27 Each inventory is used to predict the counts of another one that is matched based on group  
28 representation, biogeography, and richness. Based on examining decisive differences  
29 between the resulting likelihoods, the new models routinely outperform eight different rivals.
- 30 5. Thanks to their simplicity, grounding in non-competitive equilibrial population dynamics,  
31 and predictive power, the new approaches have considerable relevance throughout ecology.

32

## 33 **KEYWORDS**

34 half-power distribution, log series, negative binomial distribution, Poisson log normal  
35 distribution, quarter-power distribution, scaled odds distribution, Weibull distribution

## 36 1 | INTRODUCTION

37

38 The rules of community assembly are of fundamental interest to ecologists, and debate over  
39 them goes back to the conflict between the Gleasonian and Clementsian schools in the early  
40 20th century (Eliot 2007; Presley et al., 2010). Community assembly is grounded in rates of  
41 birth, death, and immigration (Kendall, 1948). Rate variation is responsible for complex  
42 patterns at local scales such as vegetational succession and predator-prey cycles. However,  
43 the rates also scale up to govern speciation and extinction processes. Thus, they indirectly  
44 control or correlate with everything that it is interesting in community ecology and  
45 macroecology, including biogeographic patterns, species-area relationships, diversity  
46 gradients, and trait distributions.

47 There may be no agreement about which assembly processes are the most important, but  
48 the business of ecology is the same as the business of science in general: establishing process  
49 by studying pattern. The problem is that there are highly distinct strategies for drawing  
50 inferences. For example, presence-absence matrices that compare assemblages may signal  
51 several processes (Leibold & Mikkelsen, 2002; Henriques-Silva et al., 2013), and species  
52 diversity patterns can likewise suggest different population processes such as colonisation  
53 and local extirpation (MacArthur & Wilson, 1963; Loreau & Mouquet, 1999).

54 While that literature is important and interesting, the common currency of community  
55 ecology is more basic: simple inventories of species found in particular locations at particular  
56 times. The problem is that isolated inventories are generally thought not to contain enough  
57 information to indicate assembly processes with any real specificity (Lawton, 1999; McGill  
58 et al., 2007; Matthews & Whittaker, 2014). This explains why authors have discussed  
59 alternative approaches such as seeing how abundance distributions, which are counts of  
60 individuals grouped into species, vary across temporal scales (Magurran, 2007) or spatial  
61 scales (Borda-de-Água et al., 2011; Antão et al., 2021).

62 In this paper, I suggest that individual real-world distributions do have the power to  
63 differentiate quite different assembly processes. In particular, I present three new and  
64 extremely simple models of population dynamics that all generate simple species abundance  
65 distributions. I show that their predicted patterns are common in tree and animal data.  
66 Importantly, the new distributions are not only plausible but distinct, so it is possible to reject  
67 their underlying models and thereby exclude their assumptions.

68 Population models have been used in this way before. For example, Kendall (1948)  
69 predicted the log series distribution of Fisher et al. (1943) with a completely random, per-  
70 capita birth-death process; MacArthur (1960) pointed out that the log normal should result if  
71 all populations grow exponentially; and Saether et al. (2013) showed how weak density  
72 dependence could also generate the log normal distribution. Meanwhile, the influential zero-  
73 sum multinomial (ZSM) distribution of Hubbell (1997, 2001) encompasses the log series and  
74 other shapes. It can be derived from a population model that makes clear assumptions about  
75 dispersal, speciation, competition, and so on.

76 These are all long-established ideas. But except for the ZSM, newer species abundance  
77 models such as those of Tokeshi (1990) have often not gained much traction. A potential  
78 exception is the gambin model of Ugland et al. (2007), which has attracted other attention  
79 (Matthews et al., 2014, 2019). This model is difficult to assess for reasons outlined later.  
80 Comparative analyses (e.g., Baldrige et al., 2016) have therefore focused on classic  
81 alternatives such as the log series (Fisher et al., 1943) and Poisson log normal (Bulmer,  
82 1974).

83 With all of this previous work, it would be natural to think that nothing more needs to be  
84 said. Don't we already have far too many models? I will argue this is not true. But even if the  
85 general theory proposed here proves superfluous, stimulating a wider discussion may better  
86 our understanding of ecological processes. In addition, the particular new models all have  
87 built-in species richness estimators that provide maximum likelihood values when the model  
88 assumptions are met. So if the theory is any good, then these estimators might see widespread  
89 application.

90

## 91 **2 | MATERIALS AND METHODS**

92

### 93 **2.1 | Workflow for deriving distributions**

94

95 Throughout this paper, I draw a distinction between two mathematical means of summarising  
96 count data: (1) rank-abundance distributions (RADs), which are simply lists of counts  
97 ordered from greatest to least; and (2) species-abundance distributions (SADs) *sensu stricto*,  
98 which are lists of counts of species sharing counts (Fisher et al., 1943). Although some  
99 researchers prefer to fit data to models by examining RADs (e.g., Hughes, 1986; Ulrich et al.,  
100 2018), I emphasise fitting data to SADs by likelihood, as done by Prado et al. (2018), for

101 reasons explained further in the discussion of the preferred fitting method. I use RADs for  
 102 illustrative purposes because it is easier to grasp them quickly.

103 A fitted SAD is just a probability mass function (PMF) in the standard statistical sense,  
 104 which is another good reason to work with SADs. As statisticians well understand, integer-  
 105 value PMFs can be derived from continuous-value cumulative distribution functions (CDF).  
 106 A general strategy is to start with a transform of a uniform random variate  $U$  into a non-  
 107 uniform random variate  $X$ :

108

$$109 \quad X = f(U) \quad (1)$$

110

111 Next,  $U$  is solved for in terms of  $x$  to yield  $U = f(X)$ . The resulting expression is just one  
 112 minus a CDF if (1) it declines monotonically to zero as  $X$  approaches infinity, and (2) it either  
 113 starts with a value of 1 when  $X = 0$  or can be scaled easily to do so. In other words, many  
 114 expressions like  $1 - f(X)$  can be CDFs:

115

$$116 \quad F_X(x) = P(X \leq x) = 1 - U = 1 - f(X) \quad (2)$$

117

118 Finally, a PMF is produced by rounding down the first differences of the CDF:

119

$$120 \quad p_X(x) = P(X = x) = [1 - f(x + 1)] - [1 - f(x)] = f(x) - f(x + 1) \quad (3)$$

121

122 where  $x$  is an integer value. The derivation of the geometric series from the exponential  
 123 distribution is then as follows:

124

$$125 \quad X = -\ln U \quad (4)$$

126

$$127 \quad F_X(x) = 1 - U = 1 - \exp(-X) \quad (5)$$

128

$$129 \quad p_X(x) = \exp(-x) - \exp[-(x + 1)] \quad (6)$$

130

131 To confirm that this yields the geometric distribution, let its governing parameter  $p = 1$   
 132  $- \exp(-\lambda)$  where  $\lambda$  governs the exponential. Suppose  $\lambda = 3$ . In R, symbolise  $\lambda$  as  $l$  and then  
 133 compute:

```

134
135 l = 3
136 p = 1 - exp(-l)
137 x = 0:9
138 exp(-l * x) - exp(-l * (x + 1))
139 dgeom(x, p)

```

140

## 141 2.2 | New equations

142

143 The exact equations for the three new distributions examined in this paper follow easily from  
 144 the workflow. First, we consider a distribution related to the discrete Weibull (Nakagawa &  
 145 Osaki, 1975), whose general form can be derived from the exponential distribution in this  
 146 way:

147

$$148 \quad X = [-\ln(U)/\lambda]^p \quad (7)$$

149

$$150 \quad F_X(x) = 1 - \exp(-\lambda x^{1/p}) \quad (8)$$

151

$$152 \quad p_X(x) = \exp(-\lambda x^{1/p}) - \exp\{-[\lambda (x + 1)^{1/p}]\} \quad (9)$$

153

154 where  $\lambda$  and  $p$  are constants, the former just being the familiar rate parameter of the  
 155 exponential distribution.

156 The specific distribution used here, called the half-power (HP), follows from setting  $p = 2$ :

157

$$158 \quad X = [-\ln(U)/\lambda]^2 \quad (10)$$

159

$$160 \quad F_X(x) = 1 - \exp(-\lambda x^{0.5}) \quad (11)$$

161

$$162 \quad p_X(x) = \exp(-\lambda x^{0.5}) - \exp\{-[\lambda (x + 1)^{0.5}]\} \quad (12)$$

163

164 The  $p = 2$  assumption is made because a very simple population dynamics model  
 165 discussed below implies this value. Assuming any other value would require burdening the  
 166 model with extra assumptions.

167 Because  $\exp(-\lambda 0^{0.5}) = 1$  and  $\exp[-(\lambda 1^{0.5})] = \exp(-\lambda)$ , this equation yields a remarkably  
 168 simple species richness estimator:

169

$$170 \quad R = S/\exp(-\lambda) \quad (13)$$

171

172 where  $R$  = estimated richness and  $S$  = the observed number of species.

173 The second distribution, called the scaled odds, uses a scaling constant  $\mu$  and has a  
 174 simplified PMF:

175

$$176 \quad X = \mu (1/U - 1) \quad (14)$$

177

$$178 \quad F_X(x) = 1 - \mu/(x + \mu) \quad (15)$$

179

$$180 \quad p_X(x) = [\mu/(x + \mu)] - [\mu/(x + 1 + \mu)]$$

181

$$182 \quad p_X(x) = 1/[(x + \mu) (x + 1 + \mu)] \quad (16)$$

183

$$184 \quad R = (\mu + 1)/\mu S \quad (17)$$

185

186 Crucially,  $1/U - 1$  can be rearranged as  $(1 - U)/U$ . This ratio is nothing other than the  
 187 gambler's odds of a random outcome – where the probability of that outcome is itself a  
 188 random uniform variate. Odds distributions range from zero to infinity, meeting the  
 189 requirement that abundances on a continuous or discrete scale must fall into that range.

190 Finally, the quarter-power distribution incorporates features of both equations.  
 191 Specifically, a modified odds component is logged, scaled, and raised to a power. The power  
 192 term could be freed to create a two-parameter model comparable to, say, the Weibull. Very  
 193 close fits to real and simulated data are seen with a power of 4, implying that the expression's  
 194 form is realistic and the constant is canonical. The constant may reflect an equilibrium state:  
 195 a different one would presumably result in unstable and transient communities. It is denoted  
 196 with the symbol  $\gamma$ :

197

$$198 \quad X = [-\ln(2/U - 1)/\gamma]^4 \quad (18)$$

199

200 Note that  $-\ln(2/U - 1)$  has bounds of zero and infinity, with a self-evident median of  $\ln 3$   
 201 and a computable mean of  $\ln 2$ . It is very important that the expressions  $-\ln(U)$ ,  $1/U - 1$ , and  
 202  $-\ln(2/U - 1)$  collectively encompass the set of simple expressions that can convert  $U$  into this  
 203 range.

204 The other equations are:

205

$$206 \quad \gamma X^{1/4} = -\ln(2/U - 1)$$

207

$$208 \quad U = 2/[\exp(-\gamma X^{1/4}) + 1] \quad (19)$$

209

$$210 \quad F_X(x) = 1 - 2/[\exp(-\gamma x^{1/4}) + 1] \quad (20)$$

211

$$212 \quad p_X(x) = 2/\{\exp[-\gamma (x + 1)^{1/4}] + 1\} - 2/[\exp(-\gamma x^{1/4}) + 1] \quad (21)$$

213

214 The richness estimate requires a little work:

215

$$216 \quad p_X(0) = 2/[\exp(-\gamma 1^{1/4}) + 1] - 2/[\exp(-\gamma 0^{1/4}) + 1]$$

217

$$218 \quad p_X(0) = 2/[\exp(-\gamma) + 1] - 1$$

219

$$220 \quad 1 - p_X(0) = 2 - 2/[\exp(-\gamma) + 1]$$

221

$$222 \quad 1 - p_X(0) = 2 \exp(-\gamma)/[\exp(-\gamma) + 1]$$

223

$$224 \quad R = [\exp(-\gamma) + 1]/[2 \exp(-\gamma)] S \quad (22)$$

225

226 It is important to stress two other things. First, unlike the log series (Fisher et al. 1943), all  
 227 of these distributions directly imply the total species richness of a community (eqns. 13, 17,  
 228 and 22). Likewise, a richness estimate can be gotten out of a Poisson log normal fit because it  
 229 too indicates the proportion of species with non-zero counts (Grøtan & Engen, 2008). There  
 230 are issues with that distribution such as its failure to remove sample size biases, its imprecise  
 231 estimates, and its poor prediction of patterns. The first two topics merit a fuller discussion



232 elsewhere. The third problem is demonstrated in the results. On a conceptual level, I take up  
233 what it means to estimate richness from an ecological sample in the discussion.

234 Second, all of the new models have a single scaling parameter and no shape parameter. In  
235 other words, they posit that all differences between species inventories stem from just two  
236 properties – the richness of the overall species pool and the number of drawn individuals.  
237 Suppose a real-world distribution is ably described by any such distribution. Then all  
238 measures that concern distributional evenness here are irrelevant, because if a shape doesn't  
239 vary, then there is nothing for an "evenness" metric to describe. I discuss later how this  
240 deduction bears on the widespread use of Hill numbers (Hill, 1973; Chao et al., 2014).

241

### 242 **2.3 | Additional distributions**

243

244 There is a large literature on species-abundance distributions in the general sense (McGill et  
245 al., 2007). I restrict my discussion to eight published models that have received substantial  
246 attention from ecologists at different points in history. (1) The geometric series distribution  
247 (Motomura, 1932) was originally applied to RADs. This application has been thought to yield  
248 unrealistic fits to data, and the model is no longer considered viable in such a form (Alroy,  
249 2015; Baldrige et al., 2016). However, its fate is different in the current analysis, which  
250 applies the distribution to SADs instead. (2) The log series (Fisher et al., 1943) is  
251 fundamental to ecology and already considered by some to be a good descriptor of many  
252 communities (Baldrige et al., 2016), especially local ones (Antão et al., 2021). This explains  
253 why it is still routinely used in biodiversity studies, including very large-scale ones (e.g.,  
254 Buzas et al., 2002; Cazzolla Gatti et al., 2022). (3) The broken stick distribution (MacArthur,  
255 1957) has a distinct theoretical basis and makes distinct predictions about the shapes of  
256 SADs, so it is investigated here even though modern studies reject it (Alroy, 2015). The  
257 remaining distributions must be considered because of their recent advocacy. (4) The Poisson  
258 log normal (PLN: Bulmer, 1974) was applied to large-scale marine data sets by Connolly et  
259 al. (2005, 2009). (5) The zero-sum multinomial (ZSM: Hubbell, 1997, 2001) is widely  
260 advocated and has long been the subject of much debate (e.g., McGill, 2003). (6) The  
261 negative binomial was explored by Connolly et al. (2009) and Connolly and Thibaut (2012)  
262 and also applied by Tovo et al. (2017) and ter Steege et al. (2020), as part of a broader study.  
263 (7) The Weibull, a standard statistical distribution, was put forth as a good description of  
264 ecological count data by Ulrich et al. (2018). I consider the discrete version of the Weibull

265 (Nakagawa & Osaki, 1975). (8) The Zipf is another classic distribution and was thought to be  
 266 a good general descriptor of ecology communities by Su (2018).

267 I put aside the gambin distribution (Ugland et al., 2007; Matthews et al., 2019) for the  
 268 same reasons as Ulrich et al. (2018): it is a heuristic pattern descriptor not based in a process  
 269 model and one that is fit by binning the data, so a direct comparison based on fitting  
 270 alternatives to proper SADs is not possible. In particular, the *gambin* R library (Matthews et  
 271 al., 2014) was not designed to fit SADs. I also do not consider niche preoccupation models  
 272 such as the ones proposed by Sugihara (1980) and Tokeshi (1990) because these RAD-based  
 273 theories are no longer endorsed, depend on strong assumptions about competition, and do not  
 274 make clear predictions about SADs.

275

## 276 **2.4 | Likelihood-based fitting method**

277

278 Fitting models to abundance distributions is a challenging problem (Connolly & Thibaut,  
 279 2012; Matthews & Whittaker 2014; Ulrich et al., 2018). Earlier researchers sought to do so  
 280 by sorting counts into  $\log_2$  bins (Preston, 1962). However, even when maximum likelihood  
 281 methods are used (McGill, 2003) this loses much information. Thus, it is impractical when  
 282 dealing with routine ecological surveys including only 10, 20 or even 30 species (Ulrich et  
 283 al., 2018). Meanwhile, directly fitting RADs (e.g., Ulrich et al., 2018) is problematic because  
 284 (1) it depends on frequentist methods such as least-squares or major axis regression; (2) there  
 285 is no way to specify an error distribution that should apply fairly to all theoretical models;  
 286 and (3) the data violate the standard statistical requirement of independence between x- and  
 287 y-values. Specifically, it is not possible to model error in ranks sensibly because stochastic  
 288 variation in counts would generate swaps in ranks. I therefore follow others (Bulmer, 1974;  
 289 Connolly et al., 2005, 2017; Connolly & Thibaut, 2012; Prado et al., 2018; Antão et al.,  
 290 2021) in evaluating model fit by computing the likelihoods of empirical SADs. Again, the  
 291 term SAD is used here for a list of counts of species sharing particular counts of individuals.

292 Before continuing, I note that the same likelihood calculation is used in this paper for two  
 293 purposes: (1) quantifying the fit of each and every rival model to any given SAD, and (2)  
 294 finding the best value of the parameters of the new models. The function is also used to fit the  
 295 broken stick, geometric series, negative binomial, and discrete Weibull, which lack trivially  
 296 computed parameters (the log series has one) and lack existing R functions that fit the  
 297 parameters by maximum likelihood (the Poisson log normal has one).

298 The math depends on first computing the independent probability  $p_i$  that a given species  
 299 will fall in its observed count class  $i$ , i.e., the likelihood. The overall likelihood is just the  
 300 product of all the  $p_i$  values for the counts (Prado et al., 2018). Of course, only the observed  
 301 counts can be predicted and the sum of  $p_i$  over all observable classes has to be 1. However,  
 302 zero counts can't be observed and do feature in the PMF equations given above. Therefore,  
 303 the  $p$  values have to be divided by  $1 - p_0$  (meaning standardised). Connolly et al. (2017, their  
 304 eqn. 8) used the same correction.

305 Connolly and Thibaut (2012) proposed a multinomial equation for fitting SADs instead of  
 306 a binomial equation. Nothing is wrong with that. However, when it comes to actual  
 307 computation the distinction is not important: the only difference between an independent-draws  
 308 equation and a multinomial equation is the inclusion of combinatorial terms made up of  $S$  and  
 309  $s_i$ . Those values are fixed, so the combinatorial terms are fixed across all possible parameter  
 310 values, leading to identical maximum likelihood solutions. Thus, users of these methods can  
 311 choose to interpret the fitting procedure as "really" based on a multinomial model if they so  
 312 choose.

313

## 314 **2.5 | Simulations of population dynamics**

315

316 Simple simulations are used to demonstrate sufficient if not necessary conditions for the  
 317 geometric series and the three new distributions to arise. The simulations each assume a  
 318 species pool of 100,000 with initial population sizes of 100, and they continue for 1000 time  
 319 steps. Death is always a binomial process, meaning that it is per-capita (based on the initial  
 320 number of adults) with a probability that any one individual will die. Counts of recruits  
 321 ("births") are randomly drawn from the Poisson distribution. Similar results can be obtained  
 322 using models that draw birth counts from the geometric series. A non-capita birth process is  
 323 assumed because the system is assumed to be either (1) open to a steady influx of propagules,  
 324 or (2) saturated with subadults that have been generated over a series of intervals instead of  
 325 arising over just one time step. Therefore, the models could apply either to open or closed  
 326 systems.

327 The geometric series model assumes that the death rate is fixed at some fraction (0.1 in the  
 328 illustrated trials), and that the Poisson parameter of the recruitment rate is a simple random  
 329 exponential variate with a rate  $\lambda$ . All the other models are variants. The half-power model  
 330 assumes that the death probability  $p$  is a function of the birth rate  $\lambda$ , specifically  $p = 1/(\lambda + 1)$ .

331 So the rates are negatively correlated: when  $1/(\lambda + 1) = 1$  or  $9$ ,  $p = 0.5$  or  $0.1$ . The odds model  
 332 assumes a fixed death probability, here  $0.5$ , and a birth probability of  $\exp(-\lambda)/\lambda$ . Finally, the  
 333 quarter-power model also assumes a uniform death rate, again illustrated as  $0.5$ , and a birth  
 334 rate of  $\lambda^3$ . In the illustrated trial, the birth rate is scaled up by  $3$  to allow comparison with the  
 335 other curves.

336 So the models assume different relationships between birth and death – but populations  
 337 must somehow stay in a viable range. How is co-existence maintained?

338 The counter-intuitive reason is that the simulations reach an equilibrium total population  
 339 size  $K$  for each species. For example, let  $p$  = the death probability and  $d$  = the expected death  
 340 count, equal to the current population size  $p n$ . Also let  $b$  = the expected birth count, equal to  
 341  $-\ln p$  in this hypothetical model. At equilibrium, then,  $d = b$  and  $p K = \ln p$ , so  $K = \ln(p)/p$ .  
 342 Below equilibrium,  $n < \ln(p)/p$  because  $n < K$  and  $K = \ln(p)/p$ . Therefore,  $d < b$ :  $n < b/p$   
 343 because  $b = \ln p$ ,  $p n < b$  by rearrangement, and  $d < b$  because  $d = p n$ . As a result,  $n$  will  
 344 climb towards  $K$ . Above  $K$ ,  $n > 1/p^2$  and  $d > b$ , so  $n$  will fall to  $K$ . Similar proofs apply to the  
 345 preceding models. They relate closely to the equilibrial theory of island biogeography  
 346 (MacArthur & Wilson, 1963), which also assumed per-capita "death" (extinction) and steady,  
 347 non-per-capita "birth" (immigration).

348 The fact that all of this is true is easily confirmed by simulation. It is highly important  
 349 because it specifically predicts that species producing more recruits in total per time step are  
 350 more common at equilibrium. There are truly "winner" and "loser" species in this paradigm,  
 351 but all of them have equilibrial population dynamics, so all of them can co-exist.

352 All of the models assumes high but predictable variance among species in recruitment  
 353 rates because of fixed differences in traits, but little variance among individuals. Models  
 354 assuming a geometric sampling process for recruitment would build in greater variance. They  
 355 are not explored in this paper because low variance may be more intuitive to many ecologists.

356

## 357 **2.6 | Empirical data**

358

359 Four large-scale data sets and one database of local-scale species inventories were used to  
 360 benchmark the distributions. Data for communities of fishes and corals spread across the  
 361 western and central Pacific were drawn from Connolly et al. (2017). A regional data set of 18  
 362 butterfly communities from Colombia was taken from C3mbita et al. (2021). Combined  
 363 abundances of trees inventoried in 1946 plots across the Amazon basin were drawn from ter

364 Steege et al. (2020). Finally, all 3257 available inventories of local tree, insect, and vertebrate  
365 communities from around the world were drawn directly from the Ecological Register  
366 database (Alroy, 2015, 2024). A large majority apply to a single trophic level and a small  
367 local area. There was no combination of inventories and multiple inventories from the same  
368 publications were allowed to be included. After discarding inventories with less than four  
369 species, a maximum count of less than four, or entirely identical counts, 3095 remained.

370

## 371 2.7 | Assessment of model fit

372

373 The fit of the 11 models to each of the local data sets was assessed by computing the  
374 corrected Akaike information criterion (AICc) for each combination (Hurvich & Tsai, 1993).  
375 Antão et al. (2021) did the same thing. The above-mentioned likelihood calculation was used  
376 as the basis of the computations, which were implemented in the *richness* R package  
377 (<https://github.com/johnalroy/richness/releases/tag/v2.4>). The Zipf and ZSM distributions  
378 were fit first using the *sads* library (Prado et al., 2018), which uses the same likelihood  
379 equation as *richness* for all of its SAD fitting. The *poilog* library (Grøtan & Engen, 2008) in  
380 combination with the *richness* function *pln* was used to fit the PLN. The other models were  
381 fit using this paper's maximum likelihood equation, as implemented in the *richness* package.

382 The AICc statistic penalises weakly for the number of parameters in a model (either one or  
383 two in all cases), so it tends to favour more complex ones. Many data sets are small in terms  
384 of both the number of species and the number of individuals, so raw AICCs can be  
385 misconstrued to indicate meaningful differences. To avoid being misled by stochastic  
386 variation in the fits, I tallied cases where differences ( $\Delta$ s) in AICCs yielded a weight of  $> 20$ ,  
387 i.e., where  $\exp(\Delta\text{AICc}/2) > 20$ .

388 Complex models are able to fit a wide range of distribution shapes by definition, but this  
389 does not necessarily mean they are good predictors of community structure. The reason is  
390 that they overfit, so they commit strongly to a pattern that may result from random variation  
391 in counts. To show whether models could generalise, I carried out more head-to-head  
392 comparisons by (1) fitting each model to each species inventory; (2) for each inventory,  
393 selecting another one that represented the same ecological group and the same biogeographic  
394 realm (ecozone) and had the most similar numbers of non-singleton and singleton species  
395 based on the sum of log ratios of those counts (with the first-encountered inventory being  
396 chosen when there was a tie); and (3) computing the log likelihoods (LLs) of the second

397 distribution based on the first one's models. The above methodology was used to obtain the  
398 likelihoods. A likelihood weight cutoff of  $> 20$ , meaning  $\exp(\Delta LL) > 20$ , was used to flag the  
399 decisive comparisons.

400

## 401 **2.7 | Multivariate ordination based on fit statistics**

402

403 Differential sampling of the range of possible SADs might skew tallies of the best  
404 distributions for the inventories. Therefore, it is more illuminating to see which shapes across  
405 the range are able to fit which distributions, and whether the new models can account for  
406 most or all of this variation. If so, then it is possible that most communities are indeed  
407 generated by processes conforming with the key assumptions: per-capita death rates that may  
408 or may not be species-specific combined with species-specific, highly variable, and not per-  
409 capita recruitment rates.

410 Principal components analysis of the LLs is used to explore the range of shapes. A level  
411 playing field has to be created to make this possible. Specifically, the average magnitude of  
412 LLs regardless of the model tracks richness and sample size, rising with both. To account for  
413 this, the LLs for each inventory are first standardised to fall in the range between the  
414 minimum and maximum. So if the LLs for three models are 10, 13, and 20, then the  
415 standardised values are 0, 0.3, and 1. Alternative approaches would depend on making strong  
416 assumptions, such as strong and linear tracking between average LLs and either richness,  
417 sample size, or both somehow combined.

418

## 419 **3 | Results**

420

### 421 **3.1 | Simulated SADs**

422

423 Patterns closely consistent with the distributions are yielded by the appropriate simulations.  
424 Fits of models to counts are almost precise (Fig. 1). The same patterns can be seen in almost  
425 every single trial – these were selected arbitrarily.

426 The geometric series (Fig. 1A) is the most general, with fixed per-capita death rates and a  
427 simple exponential distribution of birth rates. The half-power (HP) model (Fig. 1B) assumes  
428 coupling between rates. Finally, the scaled odds and quarter-power (QP) distributions assume  
429 fixed death rates and high-variance birth rates (Figs. 1C, D).

430

### 431 **3.2 | Descriptions of empirical SADs**

432

433 The QP distribution fits all for regional data sets with great accuracy (Fig. 2). The scaled  
434 odds distribution fits the Pacific coral and fish data and the Colombian tree data next-best  
435 (Figs. 2A, B, C). The log series is second-best with the composite Amazonian tree  
436 inventories (ter Steege et al., 2020), which span a huge spatial scale (Fig. 2D). Thus, it is not  
437 clear that a multi-parameter model like the negative binomial (ter Steege et al., 2020) is really  
438 needed for this data set.

439 In terms of the local-scale data, an initial vetting of the models can be based on head-to-  
440 head comparisons that yield large differences in AICcs (AICc weights  $> 20$ : Table 1). Here,  
441 the three new distributions are decisively better than the broken stick, geometric series,  
442 negative binomial, and Zipf. They also beat the zero-sum multinomial (ZSM). The QP  
443 overwhelmingly beats the log series while the others fall to it. The Poisson log normal (PLN)  
444 and Weibull fare worse again against the QP. This is a mixed result for the HP and odds, and  
445 it suggests that the QP is the strongest of all considered distributions.

446 The fair performance of the two-parameter PLN, Weibull, and ZSM models may be an  
447 artefact of (1) the AICc's weak penalisation for model complexity, (2) overfitting, and (3) the  
448 ability of complex models to mimic distributions generated by simpler processes, including  
449 those that underlie the four models emphasised here.

450

### 451 **3.3 | Predictions of empirical SADs**

452

453 The differences are much more dramatic when fitted SADs are used to predict matched SADs  
454 (Table 2). The QP distribution now trumps all of the old models at least 80% of the time  
455 when the likelihood weight is  $> 20$ . The scaled odds distribution is also strong, with a  
456 minimum win percentage of 71. The HP more or less ties the three distributions that predict  
457 gently declining, J-shaped RADs: the log series, PLN, and Weibull. The HP and Zipf also tie.

458 In sum, because accurate prediction is more important than simple description in science,  
459 the large differences in favour of all three new models, and especially QP, yield them  
460 considerable credence. This conclusion is strengthened by limiting the comparisons to  
461 complex distributions (those having highest log likelihoods across all models  $> 100$ ). This  
462 time, the QP and scaled odds respectively beat the two-parameter distributions at least 93 and

463 86% of the time in all cases. The HP also performs better, still basically tying the Zipf (45%)  
 464 but now overcoming the log series (80%), PLN (67%), and Weibull (62%).

465 There is some important variation among 13 ecological groups with respect to relative  
 466 model performance. QP is far and away the strongest, not falling below 50% in any of the 13  
 467  $\times 8 = 104$  comparisons with older models. The scaled odds distribution is also favoured  
 468 strongly, but not so much over the log series, which it usually beats about 70 – 80% of the  
 469 time. However, this ranges from 49% (mosquitoes) to 81% (birds). Support for the HP  
 470 distribution is less impressive (sometimes  $< 50\%$  in various comparisons) when it comes to  
 471 four major groups: ants, dung beetles, mosquitoes, and trees. The three insect groups often  
 472 feature steep distributions that are well-explained by the odds and QP models. There is no  
 473 obvious latitudinal pattern in the data.

474

### 475 **3.4 | Multivariate ordination patterns**

476

477 The ordination is even more interesting because it shows which shapes go with which  
 478 distributions, and thus which shapes are broadly applicable (Fig. 3). The classic J-shaped  
 479 RAD pattern is only seen at left. The other side encompasses flattened and symmetrical  
 480 RADs only well described by two classic but underlooked one-parameter distributions: the  
 481 broken stick and much more often the geometric series (red points). The log series (yellow  
 482 points) is common only at upper left, and specifically matches RADs that start with a hook  
 483 and trail off into a straight line (as illustrated).

484 Importantly, the two-parameter distributions (turquoise points) that are of so much interest  
 485 to ecologists are only common in the central zone of the space, plus part of the branch to the  
 486 right (Fig. 3). In particular, they explain some J-shaped RADs that are curved in the middle  
 487 instead of running straight. In other words, the Poisson log normal, and Weibull mostly serve  
 488 to wrap around unremarkable distributions.

489 Finally, numerous data sets fit at least one of the three new models well, with relevant  
 490 inventories (light blue points) falling almost everywhere to the left of the small "flat RAD"  
 491 zone (Fig. 3). Thus, the new distributions are jointly able to account for most shapes. They  
 492 are also distinct (Fig. 4). The HP distribution spans a wide region (dark blue points). The  
 493 odds distribution (violet points) and QP distribution (green points) split the densely-populated  
 494 left side, which includes many distributions that are J-shaped but steep. Like the Zipf, they  
 495 can fit broad distributions with hyper-abundant dominant species. But they can also account  
 496 for the straightness of the log series-type RADs.



497

## 498 **4 | Discussion**

499

### 500 **4.1 | Inference of process**

501

502 For many years, ecologists were optimistic about inferring processes from species abundance  
503 distributions (Fisher et al., 1943; MacArthur, 1957; Preston, 1962; May, 1975; Sugihara,  
504 1980; Hughes, 1986; Tokeshi, 1990; Hubbell, 2001). However, influential papers such as  
505 McGill et al. (2007) have more recently argued that because there are so many models  
506 making such similar predictions, the entire enterprise is doomed.

507 This perspective overlooks the basic logic of the current analysis: whenever a population  
508 model *M* exactly predicts a distribution *D*, rejecting *D* based on empirical data also rejects *M*.  
509 Thus, fitting SADs can be considerably informative – but only when distributions are simple  
510 and grounded in models. In fact, the three new one-parameter distributions actually do predict  
511 patterns well (Figs. 1 – 4, Tables 1 and 2). Therefore, they actually do inform us about  
512 fundamental ecological processes. By contrast, two-parameter distributions may serve no real  
513 purpose because (1) they are not needed to predict the full range of possible SADs (Fig. 3);  
514 (2) they are mostly not grounded in simple population dynamical models (as opposed to Fig.  
515 1); and (3) science operates on the principle that simple theories are better.

516 The proposed population models are ecologically interesting and important for several  
517 other major reasons. (1) All of them are not only simple, but simple variants of each other.  
518 (2) They assume high variance in recruitment rates among species but low variance among  
519 individuals within species. By contrast, the fully neutral log series model assumes no  
520 consistent, trait-based variation in demographic rates among species (Kendall, 1948; Hubbell,  
521 2001). In the new models, species do have systematically different demographic rates and  
522 equilibrium population sizes because of their traits, so there are "winners" and "losers" in  
523 perpetuity. (3) The models imply that populations reach equilibrium strictly because of  
524 demographic tradeoffs (Fig. 1). There is no role for competition, niche preoccupation,  
525 assembly rules, speciation, extinction, or any other non-local, non-random process. Thus,  
526 they are bona fide null models that are even simpler and less assumption-laden than that of  
527 Hubbell (1997, 2001).

528

### 529 **4.2 | Implications for quantifying biodiversity**

530

531 In recent years, ecologists have also moved to the idea that communities should be assessed  
532 by computing Hill numbers (Hill, 1973) such as Shannon's  $H$  and Simpson's  $D$  (Roswell et  
533 al., 2021). Chao et al. (2014) seems to have provided much momentum in this direction. Hill  
534 numbers blend information about richness and evenness, and ecologists use them in the hope  
535 that the latter can be quantified independent of sample size. But this hope may be in vain for  
536 three reasons.

537 First, blended statistics are dubious from a philosophical point of view. Statisticians prefer  
538 to develop one descriptive statistic per property. Second, evenness is a transient property of  
539 ecosystems driven by the random success of particular species in particular places at  
540 particular times. By contrast, richness is non-transient because it is governed by processes  
541 operating on geological time scales: speciation, extinction, and dispersal. Third, one-  
542 parameter distributions vary based on sampling intensity (scale) and richness but not based  
543 on shape, and Hill numbers vary meaningfully only when "evenness" varies. Because these  
544 distributions often hold, Hill numbers only indicate that some distributions are intrinsically  
545 steep and some are shallow, with this steepness being an inflexible property of no interest on  
546 its own.

547 A further motivation for the evenness-not-richness philosophy is the notion that the  
548 richness of any community is not only unknown from raw data, but unknowable in general.  
549 There are actually two arguments of this kind. The first is just that existing methods don't  
550 work because their estimates are usually either too low or highly imprecise (Roswell et al.,  
551 2021). When the assumptions of the new methods are met, their estimates cannot be greatly  
552 biased because they depend on maximum likelihood estimates of single parameters.  
553 Likewise, the arithmetic mean of a legitimately normal distribution can't be consistently  
554 biased because the mean is the maximum likelihood value of the central tendency. Although  
555 there is no room here to say much more about the matter, the fact that such estimates are  
556 accurate and precise would merit a fuller discussion elsewhere.

557 The second proposition is that the effective sampling universe is a function of the size of  
558 an inventory: the more individuals counted, the spatiotemporally larger and therefore richer  
559 the sampled community. This argument conflates two things: (1) the number of species that  
560 would be found in an infinitely large inventory, and (2) the number of species that existed in  
561 the spatiotemporal realm that encompassed the sampling point (i.e., the community). This  
562 paper's richness equations are about the latter, not the former.

563

### 564 **4.3 | Adequacy of the new analyses and models**

565

566 It has long been agreed that a comparative study of species abundance distributions must  
567 compare multiple models by investigating multiple data sets (McGill et al., 2007). However,  
568 previous analyses have tended to consider quite different and often limited sets of  
569 distributions (Hughes, 1986; Ulrich & Ollik, 2005; Ugland et al., 2007; Ulrich et al., 2010;  
570 Connolly et al., 2014; Matthews et al., 2014, 2019; Alroy, 2015; Baldrige et al., 2016; Su,  
571 2018; Antão et al., 2021). Many have included one version or another of both the log normal  
572 and log series (e.g., Antão et al., 2021), if not always (e.g., Su, 2018). For example, the log  
573 series is a special case of the negative binomial (Fisher et al., 1943) and the latter has been  
574 tested against the Poisson log normal (Connolly et al., 2014). Past that, coverage is eclectic.

575 Thus, few studies are comparable to this one. In the face of this comprehensiveness,  
576 support for the new distributions is jointly clear when one considers their ability to predict  
577 new sets of counts from old ones (Table 2, Figs. 3, 4). It is reasonable to ask whether  
578 additional one-parameter distributions might also be sound from both a descriptive view  
579 (Table 1) and a predictive view (Table 2). But only the geometric series and log series come  
580 even close to passing both of these tests. The latter is profoundly skeptical because it assumes  
581 that communities are drawn from pools with infinite richness (Fisher et al., 1943). It also  
582 assumes that species are identical in terms of population dynamics, in which respect it may  
583 take null modelling a bit too far. After all, this assumption discards the entire premise of trait-  
584 based ecology. Thus, the three newly proposed distributions are not only jointly adequate but  
585 arguably more sensible. One way or another, it is fair to suggest that the structure of many or  
586 even most communities does actually result from extremely simple dynamical processes.

587

### 588 **Acknowledgments**

589

590 I thank Michael Foote, Matthew Kosnik, and colleagues at Macquarie University, the  
591 University of Nebraska, Lincoln, and the University of Tasmania for helpful discussions.  
592 Hans ter Steege and Werner Ulrich commented on the text. The author is the recipient of a  
593 Discovery Project Award (project number DP210101324) funded by the Australian  
594 Government.

595

### 596 **Conflict of interest statement**

597

598 The author has no conflict of interest to declare.

599

### 600 **Data availability statement**

601

602 The data are available from the Dryad digital repository  
603 (<https://datadryad.org/stash/dataset/doi:10.5061/dryad.br15dvdc>).

604

### 605 **References**

606

607 Alroy, J. (2010). The shifting balance of diversity among major marine animal groups.  
608 *Science*, 329, 1191-1194.

609 Alroy, J. (2015). The shape of terrestrial abundance distributions. *Science Advances*, 1,  
610 e1500082.

611 Alroy, J. (2024). Data from: three models of ecological community assembly: terrestrial  
612 species inventories. *Dryad*. <https://doi.org/10.5061/dryad.br15dvdc>

613 Antão, L. H., Magurran, A. E., & Dornelas, M. (2021). The shape of species abundance  
614 distributions across spatial scales. *Frontiers in Ecology and Evolution*, 9, 626730.  
615 <https://doi.org/10.3389/fevo.2021.626730>

616 Baldridge, E., Harris, D. J., Xiao, X., & White, E. P. (2016). An extensive comparison of  
617 species-abundance distribution models. *PeerJ*, 4, e2823.

618 Borda-de-Água, L., Borges, P. A. V., Hubbell, S. P., & Pereira, H. M. (2011). Spatial scaling  
619 of species abundance distributions. *Ecography*, 35, 549-556.

620 Bulmer, M. G. (1974). On fitting the Poisson lognormal distribution to species-abundance  
621 data. *Biometrics*, 30, 101-110.

622 Buzas, M. A., Collins, L. S., & Culver, S. J. (2002). Latitudinal difference in biodiversity  
623 caused by higher tropical rate of increase. *Proceedings of the National Academy of  
624 Sciences USA*, 99, 7841-7843.

625 Cazzolla Gatti, R. et al. (2022). The number of tree species on Earth. *Proceedings of the  
626 National Academy Sciences USA*, 119, e2115329119.

627 Chao, A. (1984). Nonparametric estimation of the number of classes in a population.  
628 *Scandinavian Journal of Statistics*, 11, 265- 270.

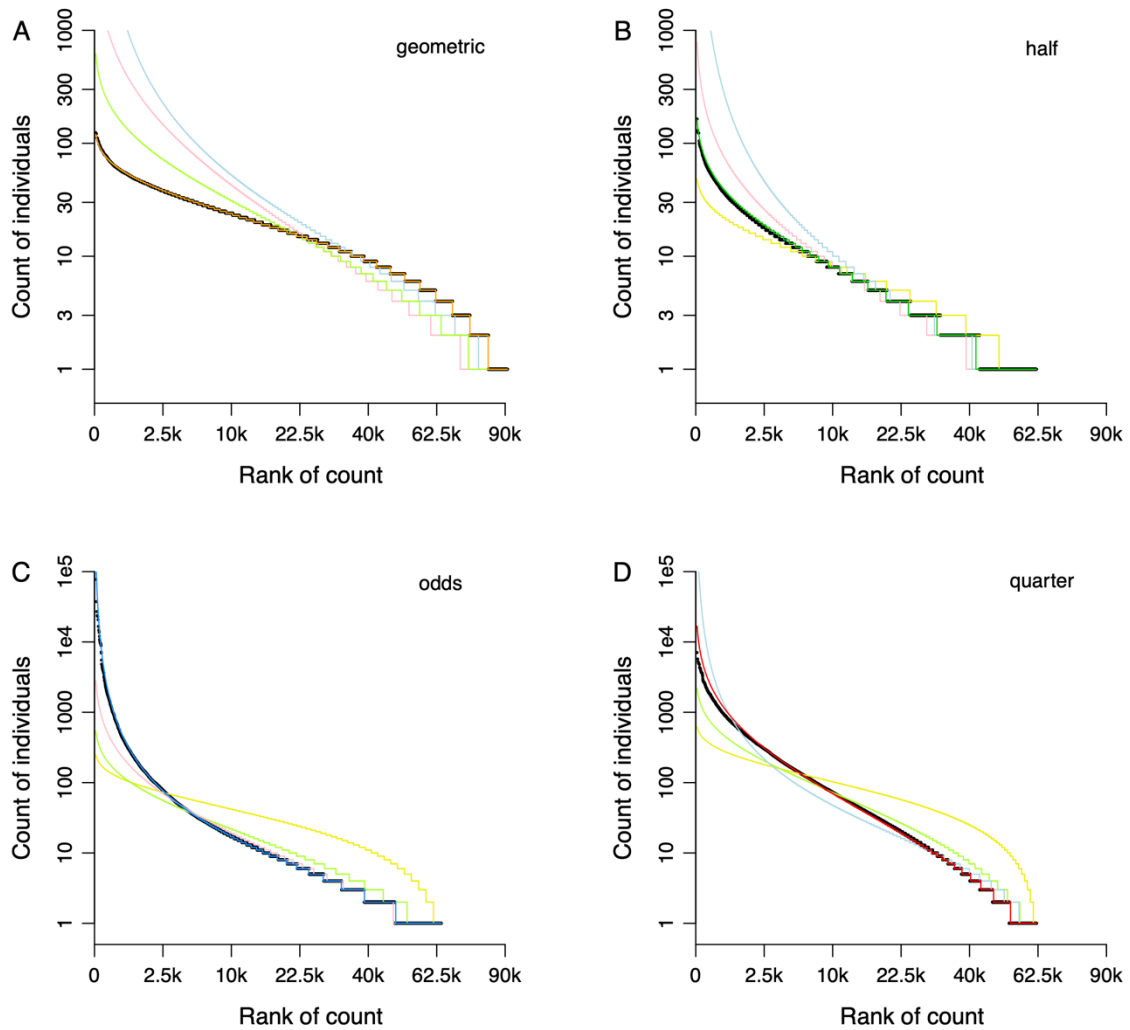
- 629 Chao, A., Gotelli, N. J., Hsieh, T. C., Sander, E. L., Ma, K. H., Colwell, R. K., & Ellison, A.  
630 M. (2014). Rarefaction and extrapolation with Hill numbers, a framework for sampling  
631 and estimation in species diversity studies. *Ecological Monographs*, 84, 45-67.
- 632 C3mbita, J. L., Giraldo, C. E., & Escobar, F. (2021). Data from: Environmental variation  
633 associated with topography explains butterfly diversity along a tropical elevation gradient,  
634 Dryad, Dataset, <https://doi.org/10.5061/dryad.vx0k6djsn>.
- 635 Connolly, S. R., et al. (2014). Commonness and rarity in the marine biosphere. *Proceedings*  
636 *of the National Academy of Sciences USA*, 111, 8524-8529.
- 637 Connolly, S. R., Dornelas, M., Bellwood, D. R., & Hughes, T. P. (2009). Testing species  
638 abundance models, a new bootstrap approach applied to Indo-Pacific coral reefs. *Ecology*,  
639 90, 3138-3149.
- 640 Connolly, S. R., Hughes, T. P., & Bellwood, D. R. (2017). A unified model explains  
641 commonness and rarity on coral reefs. *Ecology Letters*, 20, 477-486.
- 642 Connolly, S. R., Hughes, T. P., Bellwood, D. R., & Karlson, R. H. (2005). Community  
643 structure of corals and reef fishes at multiple scales. *Science*, 309, 1363-1365.
- 644 Connolly, S. R., & Thibaut, L. M. (2012). A comparative analysis of alternative approaches  
645 to fitting species-abundance models. *Journal of Plant Ecology*, 5, 32-45.
- 646 Eliot, C. (2007). Method and metaphysics in Clements's and Gleason's ecological  
647 explanations. *Studies in History and Philosophy of Science C*, 38, 85-109.
- 648 Fisher, R.A., Corbet, A.S., & Williams, C.B. (1943). The relation between the number of  
649 species and the number of individuals in a random sample of an animal population.  
650 *Journal of Animal Ecology*, 12, 42– 58.
- 651 Gr3tan, V., & Engen, S. (2008). poilog: Poisson lognormal and bivariate Poisson lognormal  
652 distribution. R package version 0.4.
- 653 Henriques-Silva, R., Lindo, Z., & Peres-Neto, P. R. (2013). A community of  
654 metacommunities: exploring patterns of species distributions across large geographical  
655 areas. *Ecology*, 94, 627-639.
- 656 Hill, M. O. (1973). Diversity and evenness: a unifying notation and its consequences.  
657 *Ecology*, 54, 627-639.
- 658 Hubbell, S. P. (1997). A unified theory of biogeography and relative species abundance and  
659 its application to tropical rain forests and coral reefs. *Coral Reefs*, 16, S9-S21.
- 660 Hubbell, S. P. (2001). *The unified neutral theory of biodiversity and biogeography*. Princeton  
661 University Press.

- 662 Hughes, R. G. (1986). Theories and models of species abundance. *American Naturalist*, 128,  
663 879-899.
- 664 Hurvich, C. M., & Tsai, C. L. (1993). A corrected Akaike information criterion for vector  
665 autoregressive model selection. *Journal of Time Series Analysis*, 14, 271-279.
- 666 Kendall, D. G. (1948). On some modes of population growth leading to R. A. Fisher's  
667 logarithmic series distribution. *Biometrika*, 35, 6-15.
- 668 Lawton, J. H. (1999). Are there general laws in ecology? *Oikos*, 84, 177-192.
- 669 Leibold, M. A., & Mikkelsen, G. M. (2002). Coherence, species turnover, and boundary  
670 clumping: elements of metacommunity structure. *Oikos*, 97, 237-250.
- 671 Loreau, M., & Mouquet, N. (1999). Immigration and the maintenance of local species  
672 diversity. *American Naturalist*, 154, 427-440.
- 673 MacArthur, R. H. (1957). On the relative abundance of bird species. *Proceedings of the*  
674 *National Academy of Sciences USA*, 43, 293-295.
- 675 MacArthur, R. H. (1960). On the relative abundance of species. *American Naturalist*, 94, 25-  
676 36.
- 677 MacArthur, R. H., & Wilson, E. O. (1963). An equilibrium model of insular zoogeography.  
678 *Evolution*, 17, 373-387.
- 679 Magurran, A. E. (2007). Species abundance distributions over time. *Ecology Letters*, 10, 347-  
680 354.
- 681 Matthews, T. J., Borregaard, M. K., Gillespie, C. S., Rigal, F., Ugland, K. I., Ferreira Krüger,  
682 R., Marques, R., Sadler, J. P., Borges, P. A. V., Kubota, Y., & Whittaker, R. J. (2019).  
683 Extension of the gambin model to multimodal species abundance distributions. *Methods in*  
684 *Ecology and Evolution*, 10, 432-437.
- 685 Matthews, T. J., Borregaard, M. K., Ugland, K. I., Borges, P. A. V., Rigal, F., Cardoso, P., &  
686 Whittaker, R. J. (2014). The gambin model provides a superior fit to species abundance  
687 distributions with a single free parameter: evidence, implementation and interpretation.  
688 *Ecography*, 37, 1002-1011
- 689 Matthews, T. J., & Whittaker, R. J. (2014). Fitting and comparing competing models of the  
690 species abundance distribution: assessment and prospect. *Frontiers of Biogeography*, 6,  
691 67-82.
- 692 May, R. M. (1975). Patterns of species abundance and diversity. In M. L. Cody & J. M.  
693 Diamond (Eds.), *Ecology and evolution of communities*. Belknap.
- 694 McGill, B. J. (2003). A test of the unified neutral theory of biodiversity. *Nature*, 422, 881-  
695 885.

- 696 McGill, B.J., Etienne, R.S., Gray, J.S., Alonso, D., Anderson, M.J., Benecha, H.K., et al.  
697 (2007). Species abundance distributions: moving beyond single prediction theories to  
698 integration within an ecological framework. *Ecology Letters*, 10, 995– 1015.
- 699 Motomura, I. (1932). A statistical treatment of associations. *Japanese Journal of Zoology*, 44,  
700 379-383.
- 701 Nakagawa, R., & Osaki, S. (1975). The discrete Weibull distribution. *IEEE Transactions on*  
702 *Reliability*, 24, 300-301.
- 703 Prado, P. I., Dantas Miranda, M., & Chalom, A. (2018). sads: maximum likelihood  
704 models for species abundance distributions. R package version 0.4.2.
- 705 Presley, S. J., Higgins, C. L., & Willig, M. R. (2010). A comprehensive framework for the  
706 evaluation of metacommunity structure. *Oikos*, 119, 908-917.
- 707 Preston, F. W. (1962). The canonical distribution of commonness and rarity of species.  
708 *Ecology*, 43, 410-432.
- 709 Roswell, M., Dushoff, J., & Winfree, R. (2021). A conceptual guide to measuring species  
710 diversity. *Oikos*, 130, 321-338.
- 711 Saether, B. E., Engen, S., & Grøtan, V. (2013). Species diversity and community similarity in  
712 fluctuating environments: parametric approaches using species abundance distributions.  
713 *Journal of Animal Ecology*, 82, 721-738.
- 714 Su, Q. (2018). A general pattern of the species abundance distribution. *PeerJ*, 6, e5928.
- 715 Sugihara, G. (1980). Minimal community structure: an explanation of species abundance  
716 patterns. *American Naturalist*, 116, 770-787.
- 717 ter Steege, H. et al. (2020). Biased-corrected richness estimates for the Amazonian tree flora.  
718 *Scientific Reports*, 10, 10130.
- 719 Tokeshi, M. (1990). Niche apportionment or random assortment: species abundance patterns  
720 revisited. *Journal of Animal Ecology*, 59, 1129-1146.
- 721 Tovo, A., Suweis, S., Formentin, M., Favretti, M., Volkov, I., Banavar, J. R., Azaele, S., &  
722 Maritan, A. (2017). Upscaling species richness and abundances in tropical forests. *Science*  
723 *Advances*, 3, e1701438.
- 724 Ugland, K. I., Lamshead, P. J. D., McGill, B., Gray, J. S., O'Dea, N., Ladle, R. J., &  
725 Whittaker, R. J. (2007). Modelling dimensionality in species abundance distributions:  
726 description and evaluation of the Gambin model. *Evolutionary Ecology Research*, 9, 313-  
727 324.

- 728 Ulrich, W., Nakadai, R., Matthews, T. J., & Kubota, Y. (2018). The two-parameter Weibull  
729 distribution as a universal tool to model the variation in species relative abundances.  
730 *Ecological Complexity*, 36, 110-116.
- 731 Ulrich, W., & Ollik, M. (2005). Limits to the estimation of species richness: the use of  
732 relative abundance distributions. *Diversity and Distributions*, 11, 265-273.
- 733 Ulrich, W., Ollik, M., & Uglan, K. I. (2010). A meta-analysis of species-abundance  
734 distributions. *Oikos*, 119, 1149-1155.
- 735

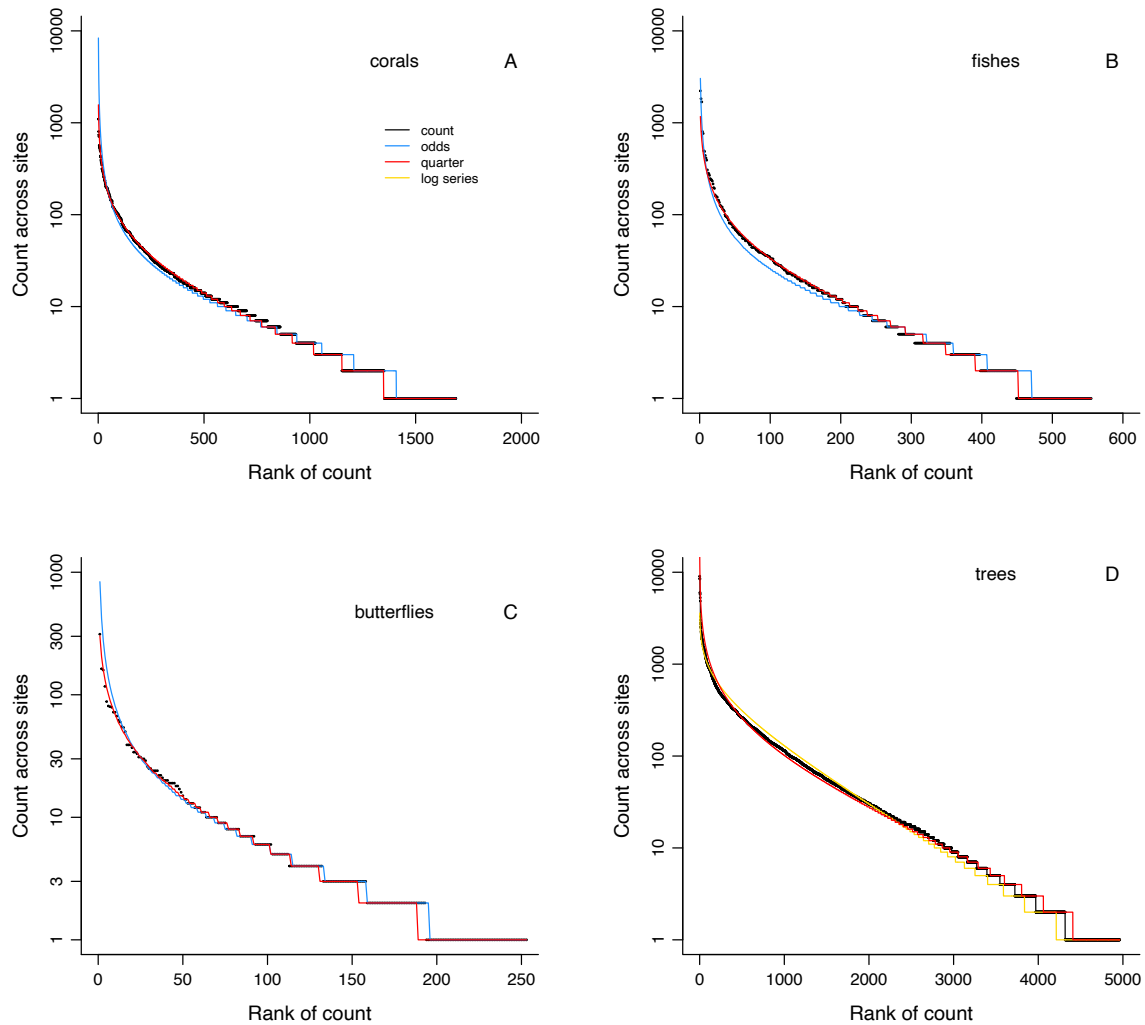




736

737

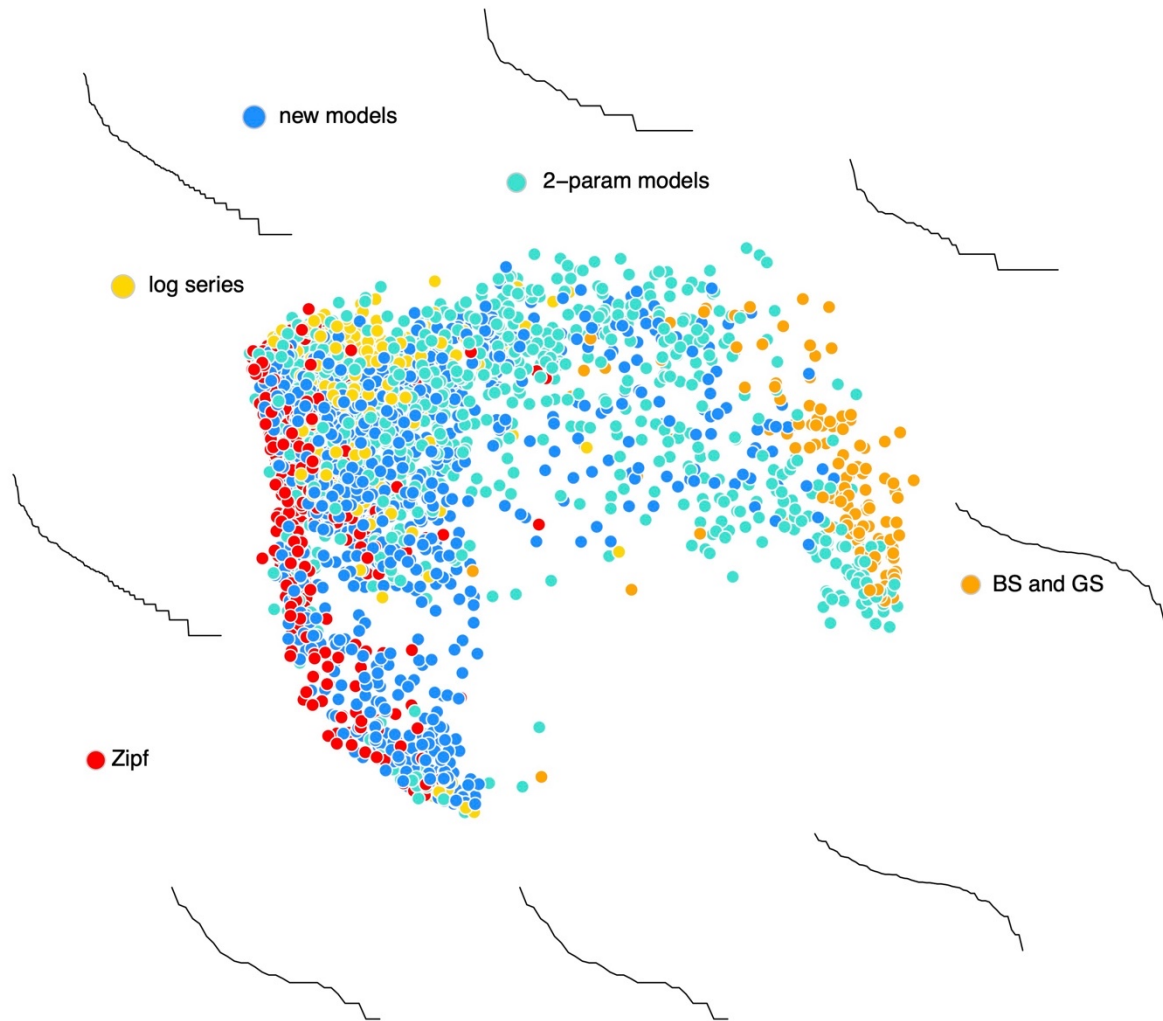
738 Figure 1. Simulated rank-abundance distributions for pools of 100,000 species. Curves show  
 739 the raw counts (black lines), geometric series (orange lines), half-power (half) distribution  
 740 (green lines), scaled odds distribution (blue lines), and quarter-power distribution (red lines).  
 741 Distributions best-fitting a given model are illustrated in bolder colours. x-axes are square-  
 742 root transformed; y-axes are log transformed. Recruitment ("birth") counts in each time step  
 743 follow a Poisson distribution; death counts follow a binomial distribution. Birth rates vary  
 744 exponentially. (A) Geometric series: the death probability is fixed at 0.1. (B) Half-power  
 745 model: the death probability is the birth rate  $\lambda$  rescaled as  $1/(\lambda + 1)$ . (C) Scaled odds model:  
 746 the death probability is 0.5 and the birth rate is  $\exp(-\lambda)/\lambda$ . (D) Quarter power model: the  
 747 death probability is 0.5 and the birth rate is  $\lambda^3$ .



748

749

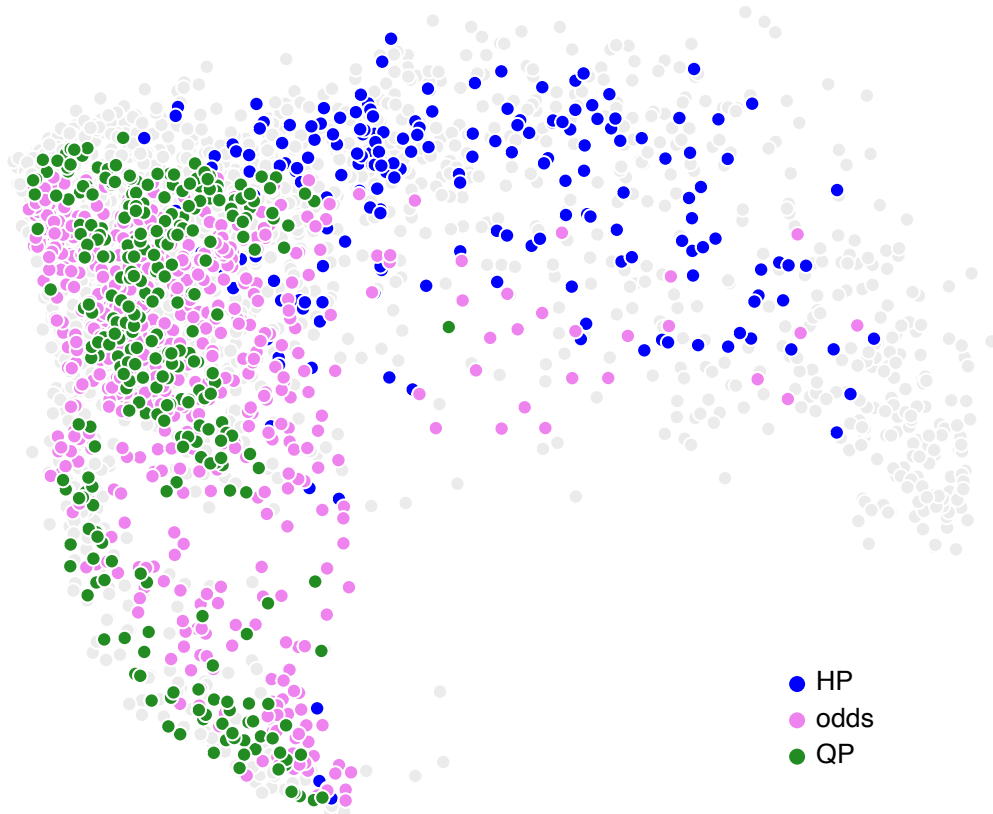
750 Figure 2. Examples of regional rank-abundance distributions. Black lines; raw counts; light  
 751 blue lines: scaled odds distribution; red lines: quarter-power distribution; yellow line in (D):  
 752 log series. The best two distributions in each case are illustrated: the quarter-power model is  
 753 always best. (A) Corals from the Pacific Ocean (Connolly et al., 2017). Scaled odds is  
 754 second. (B) Fishes from the Pacific Ocean (Connolly et al., 2017). Odds is second. (C)  
 755 Butterflies from Colombia (Cómbita et al., 2021). Odds is second. (D) Trees from Amazonia  
 756 (ter Steege et al., 2020). Log series is second.



757

758

759 Figure 3. Ordination of species inventories based on the fits of 11 models. Points closer  
 760 together yield similar log likelihoods. Likelihoods are produced by fitting models to  
 761 inventories and using the fits to predict distributions for other inventories matched by  
 762 considering ecological groups, biogeographic regions, and species counts (see text). Data  
 763 come from the Ecological Register (Alroy, 2015, 2024). Eight lines at the edges illustrate  
 764 representative rank-abundance distributions each including at least 30 species. Point colours  
 765 indicate the models that best fit each inventory's data. Blue = the three new methods (half-  
 766 power exponential, scaled odds, and quarter-power); turquoise = two-parameter models  
 767 (negative binomial, Poisson log normal, Weibull, and zero-sum multinomial); orange = flat  
 768 one-parameter models (BS = broken stick and GS = geometric series); red = the Zipf model;  
 769 yellow = the log series. See the text for references.



770

771

772 Fig. 4. Ordination of species inventories highlighting the newly proposed distribution models.

773 Data and methods are the same as in Fig. 3. Colours indicate the best models. HP = half-

774 power (blue points); odds = scaled odds (violet); QP = quarter-power (green). Points best

775 fitting the other distributions are in grey.



776 Table 1. Head-to-head comparisons of 11 species abundance distribution models. Each pair  
 777 of numbers shows how many published terrestrial ecological inventories are better fit to the  
 778 column's distribution than the row's distribution according to the corrected Akaike  
 779 information criterion (Hurvich & Tsai, 1993) with a weight > 20. Proportions > 0.5 are in  
 780 bold. Data are local-scale inventories drawn from the Ecological Register and repositied on  
 781 Dryad (Alroy, 2024). Models are explained and referenced in the text. HP = half-power; odds  
 782 = scaled odds; QP= quarter power; geom. series = geometric series; n. binomial = negative  
 783 binomial; PLN = Poisson log normal; ZSM = zero-sum multinomial.

784

	HP	odds	QP	broken stick	geom. series	log series
HP		<b>222/391</b>	<b>297/390</b>	84/1875	74/1711	<b>228/346</b>
odds	169/391		<b>195/277</b>	134/1818	119/1653	<b>316/510</b>
QP	93/390	82/277		202/1914	188/1777	20/130
broken stick	<b>1797/1875</b>	<b>1684/1818</b>	<b>1712/1914</b>		<b>389/396</b>	<b>1755/1947</b>
geom. series	<b>1637/1711</b>	<b>1534/1653</b>	<b>1589/1777</b>	7/396		<b>1633/1814</b>
log series	118/346	194/510	<b>110/130</b>	192/1947	181/1814	
Zipf	<b>1711/1878</b>	<b>1538/1606</b>	<b>1748/1773</b>	897/2181	953/2104	<b>1811/1864</b>
n. binomial	<b>1911/1952</b>	<b>1678/1723</b>	<b>1803/1889</b>	821/1400	931/1373	<b>1899/1996</b>
PLN	236/478	<b>246/465</b>	<b>247/394</b>	195/1746	195/1610	<b>301/512</b>
Weibull	178/468	179/436	<b>158/316</b>	162/1751	167/1624	170/389
ZSM	<b>474/621</b>	<b>575/755</b>	<b>390/400</b>	455/2017	468/1907	<b>144/145</b>

785

	Zipf	n. binomial	PLN	Weibull	ZSM
HP	167/1878	41/1952	<b>242/478</b>	<b>290/468</b>	147/621
odds	68/1606	45/1723	219/465	<b>257/436</b>	180/755
QP	25/1773	86/1889	147/394	<b>158/316</b>	10/400
broken stick	<b>1284/2181</b>	579/1400	<b>1551/1746</b>	<b>1589/1751</b>	<b>1562/2017</b>

geom. series	<b>1151/2104</b>	442/1373	<b>1415/1610</b>	<b>1457/1624</b>	<b>1439/1907</b>
log series	53/1864	97/1996	211/512	<b>219/389</b>	1/145
Zipf		482/1460	<b>1296/1437</b>	<b>1352/1419</b>	<b>1159/1326</b>
n. binomial	<b>978/1460</b>		<b>1316/1328</b>	<b>1371/1375</b>	<b>1351/1500</b>
Poisson LN	141/1437	12/1328		<b>88/115</b>	80/446
Weibull	67/1419	4/1375	27/115		3/375
ZSM	167/1326	149/1500	<b>366/446</b>	<b>372/375</b>	

786

787

788 Table 2. Head-to-head comparisons of 11 species abundance distribution models based on  
 789 predictions of counts in matched inventories. Each model is fitted to each inventory in the  
 790 overall Ecological Register data set (Alroy, 2024) and then projected onto another inventory  
 791 with similar singleton and non-singleton species counts that represents the same ecological  
 792 group and ecozone. Each pair of numbers shows how many inventories better fit to the  
 793 column's distribution than the row's distribution according to the log likelihood of the second  
 794 count vector, with a relative weight > 20. Proportions > 0.5 are in bold. Data and models are  
 795 explained and referenced in the text; abbreviations are as in Table 1.

796

	HP	odds	QP	broken stick	geom. series	log series
HP		<b>643/781</b>	<b>680/710</b>	22/2321	26/2100	232/576
odds	138/781		<b>209/380</b>	20/2247	45/2019	265/902
QP	30/710	171/380		44/2307	57/2097	43/611
broken stick	<b>2299/2321</b>	<b>2227/2247</b>	<b>2263/2307</b>		<b>1291/1292</b>	<b>2273/2318</b>
geom. series	<b>2074/2100</b>	<b>1984/2029</b>	<b>2040/2097</b>	1/1292		<b>2055/2114</b>
log series	<b>344/576</b>	<b>637/902</b>	<b>568/611</b>	45/2318	59/2114	
Zipf	<b>661/1256</b>	<b>730/923</b>	<b>756/949</b>	215/2265	313/2120	<b>650/1152</b>
n. binomial	<b>1677/1697</b>	<b>1652/1678</b>	<b>1732/1769</b>	188/1494	625/1433	<b>1738/1777</b>
Poisson LN	<b>459/841</b>	<b>508/692</b>	<b>544/634</b>	56/2290	139/2036	<b>474/770</b>
Weibull	414/834	<b>525/739</b>	<b>525/609</b>	32/2272	155/2023	<b>378/725</b>
ZSM	<b>734/930</b>	<b>911/1172</b>	<b>859/908</b>	37/2314	330/2086	<b>642/644</b>

797

	Zipf	n. binomial	PLN	Weibull	ZSM
HP	595/1256	20/1697	382/841	420/834	196/930
odds	193/923	26/1678	184/692	218/739	261/1172
QP	193/949	37/1769	90/634	84/609	49/908
broken stick	<b>2050/2265</b>	<b>1306/1494</b>	<b>2234/2290</b>	<b>2240/2272</b>	<b>2277/2314</b>



geom. series	<b>1807/2120</b>	<b>808/1433</b>	<b>1897/2036</b>	<b>1868/2023</b>	<b>1756/2086</b>
log series	502/1152	39/1777	296/770	347/725	2/644
Zipf		201/1654	<b>715/1243</b>	<b>719/1245</b>	662/1468
n. binomial	<b>1453/1654</b>		<b>1652/1706</b>	<b>1607/1682</b>	<b>1437/1775</b>
PLN	528/1243	54/1706		<b>283/532</b>	252/983
Weibull	526/1245	75/1682	249/532		245/986
ZSM	<b>806/1468</b>	338/1755	<b>731/983</b>	<b>741/986</b>	